A ms submitted to *Science of the Total Environment*

(preprint available in *BioRxiv* https://doi.org/10.1101/712570)

Revised v2. 12 August 2021

Diel dynamics of dissolved organic matter and heterotrophic prokaryotes reveal enhanced growth at the ocean's mesopelagic fish layer during daytime

Xosé Anxelu G. Morán[1*], Francisca C. García[1,2], Anders Røstad[1], Luis Silva[1], Najwa Al-Otaibi[1,3], Xabier Irigoien[4], Maria L. Calleja[1,5]

[1]King Abdullah University of Science and Technology (KAUST), Red Sea Research Center, Biological and Environmental Science & Engineering Division, 23955-6900 Thuwal, Saudi Arabia

[2]Environment and Sustainability Institute, University of Exeter, TR10 9FE Penryn, United Kingdom

[3]Department of Biology, Taif University, 26571 Taif, Saudi Arabia

[4]AZTI Tecnalia, 20110 Pasaia, Spain

[5]Max Planck Institute for Chemistry, 55128 Mainz, Germany

*Corresponding Author. Email: xelu.moran@kaust.edu.sa , xelu.moran@ieo.es
Present address: Instituto Español de Oceanografía, Centro Oceanográfico de Gijón/Xixón, 33212 Gijón/Xixón, Spain

ABSTRACT

Contrary to epipelagic waters, where biogeochemical processes closely follow the light and dark periods, little is known about diel cycles in the ocean's mesopelagic realm. Here, we monitored the dynamics of dissolved organic matter (DOM) and planktonic heterotrophic prokaryotes every 2 h for one day at 0 and 550 m (a depth occupied by vertically migrating fishes during light hours) in oligotrophic waters of the central Red Sea. We additionally performed predator-free seawater incubations of samples collected from the same site both at midnight and at noon. Comparable in situ variability in microbial biomass and dissolved organic carbon concentration suggests a diel supply of fresh DOM in both layers. The presence of fishes in the mesopelagic zone during daytime likely promoted a sustained, longer growth of larger prokaryotic cells. The specific growth rates were consistently higher in the noon experiments from both depths (surface: 0.34 vs. 0.18 d^{-1}, mesopelagic: 0.16 vs. 0.09 d^{-1}). Heterotrophic prokaryotes in the mesopelagic layer were also more efficient at converting extant DOM into new biomass. These results suggest that the ocean's twilight zone receives a consistent diurnal supply of labile DOM from diel vertical migrating fishes, enabling an unexpectedly active community of heterotrophic prokaryotes.

Keywords: diel cycles, marine biogeochemistry, fish-heterotrophic prokaryotes interactions, mesopelagic, Red Sea

1. INTRODUCTION

Planktonic heterotrophic prokaryotes (HP) pertaining to the domains Bacteria and Archaea rely on labile dissolved organic matter (DOM) for metabolism and growth (Carlson et al., 1994; Goldman et al., 2000; Pomeroy et al., 2007). In surface waters, diel cycles in HP biomass and activity have been related to the photosynthetic activity of phytoplankton (Gasol et al., 1998), which obviously follows sunlight. Heterotrophic prokaryotes dependence on DOM derived from planktonic algae (Baines and Pace, 1991) was reported to increase offshore, far from coastal inputs, in temperate and polar ecosystems (Morán et al., 2002). Although this relationship, also known as bacterioplankton-phytoplankton coupling, has been the subject of debate (Fouilland and Mostajir, 2010; Morán and Alonso-Sáez, 2011), in regions with low DOM advection (e.g., at permanently stratified sites without anthropogenic or riverine inputs nearby, such as oligotrophic tropical waters), we might expect strong diel signals in the response of heterotrophic prokaryotes coupled to the activity of primary producers (Ruiz-González et al., 2012). In this regard, the Red Sea offers a unique opportunity to study biogeochemical processes in oligotrophic ecosystems. With no permanent rivers, the only allochthonous inputs of DOM come from urban centers such as Suez, Ghardaqa, Jeddah or Port Sudan, coastal macrophytes (Alongi and Mukhopadhyay, 2015; Duarte and Cebrián, 1996) or dust events (Bao et al., 2018; Lekunberri et al., 2019).

While epipelagic processes driven by primary production are well known (Herndl and Reinthaler, 2013; Henson et al., 2012), large gaps in our understanding of the ecology and biogeochemistry of the mesopelagic zone (i.e., waters between 200 m and 1000 m) remain (Robinson et al., 2010). In the mesopelagic realm, trophic interactions between microbes and metazoa have been long neglected. The available studies have focused mostly on mesozooplankton (Bianchi et al., 2013b; Isla et al., 2015; Al-Mutairi and Landry, 2001). However, recent reports on the large biomass contributed to the ocean's biota by mesopelagic fishes performing diel vertical migration (DVM) suggest they may also play an important role as rapid vectors of labile organic mater (Klevjer et al., 2016; Irigoien et al., 2014; Wang et al., 2019). DVM can affect only a fraction of individuals from a given population (Klevjer et al., 2016). In the Red Sea, virtually the entire populations of mesopelagic fishes migrate daily

between the surface and the so-called deep scattering layer (DSL) usually located between 400 and 650 m in the mesopelagic zone (Klevjer et al., 2012; Røstad et al., 2016). DVM fishes have been recently suggested to generate hotspots for heterotrophic prokaryotes, yielding significantly higher bacterial growth efficiencies compared with shallower layers (Calleja et al., 2018). An analysis of a 24 h intensive sampling at the same location has supported the existence of diel inputs of labile DOM fueling the HP community at the depths occupied by mesopelagic fishes during daytime (García et al., 2018). Both DOC concentrations and high nucleic acid content (HNA) bacteria and archaea, usually made up of copiotrophic taxa (Vila-Costa et al., 2012; Schattenhofer et al., 2011) and more active than the low nucleic acid content (LNA) group (Gasol et al., 1999; Bouvier et al., 2007; Morán et al., 2011), fluctuated as widely in waters below 200 m as in the upper layers. However, for the hypothesis of the mesopelagic labile DOM hotspots to be true, we should be able to demonstrate that the presence or absence of fishes in the twilight zone does indeed make a difference.

Here, we report on the results of two short-term incubations with water collected from the epi- and mesopelagic layers (surface and 550 m, respectively) of the central Red Sea at midnight and at the following midday. After removing protistan grazers and other larger organisms by filtration, we followed the dynamics of DOM-heterotrophic prokaryotes interactions for 8 days. In parallel, we conducted a high frequency (every 2 h for a full 24 h starting at noon) characterization of the same depths, focusing on the response of heterotrophic prokaryotes abundance, cell size and biomass to changes in DOM concentrations including its fluorescent properties, previously unreported for this basin. The specific objectives of this study were: i) to assess the diurnal scales of variability in the standing stocks of HP and DOM in epipelagic and mesopelagic waters of the central Red Sea, and ii) to test for differences in the specific growth rate, maximum biomass and growth efficiency of HP between nighttime and daytime in both layers. Our hypotheses are that differences over 24 h at the surface would follow phytoplankton photosynthesis and that DOM supplied by DVM fishes in the mesopelagic zone during the day had a commesurable effect on the above-mentioned variables. Rather than purely comparing the surface and the DSL, subject to different DOM synthesis and

transformation processes, our objective was to detect differences between day and night values within each layers.

2. METHODS

2.1. Environmental sampling

We occupied one station located 13.4 km offshore to the northwest of King Abdullah Economic City, Saudi Arabia (lat 22.46°N, lon 39.02°E, Calleja et al., 2018; García et al., 2018) between midday March 6th and midday March 7th, 2016. In situ monitoring and sampling was conducted on board of RV Thuwal. Continuous acoustic measurements in order to locate the position of the vertically migrating mesopelagic fishes and the DSL were recorded with a Simrad EK60 38 kHz echosounder mounted on the ship's hull. From noon on March 6th until the same time on the following day we conducted CTD casts every 2 hours. At each cast we sampled discrete depths in the water column with Niskin bottles mounted on a Rosette sampler, ranging from the surface to 650 m depth. Water filtered through pre-combusted Whatman GF/F filters was collected at every other cast (7 in total) for analyzing DOC bulk concentrations and fluorescent DOM (FDOM) properties (40 mL pre-combusted glass vials) and inorganic nutrient concentrations (see Calleja et al., 2019 for details). Unfiltered water was collected at each of the 13 CTD casts for characterizing the community of heterotrophic prokaryotes (2 mL cryovials).

Hourly in situ apparent DOC production and consumption rates were estimated as the largest difference between DOC concentration in consecutive sampling times that showed an increase and decrease, respectively.

2.2. Experimental incubations

10 L of seawater from the surface and 550 m depth were collected in the midnight and noon casts on March 7th for conducting the experimental incubations of DOC consumption, change in FDOM and heterotrophic prokaryotes biomass response. In order of remove protistan grazers and planktonic organisms larger than bacteria and archaea, water was gently

filtered through pre-combusted Whatman GF/C filters (142 mm, nominal pore size 1.2 µm) and used to fill 3 x 2 L acid-cleaned polycarbonate bottles, which were subsequently incubated mimicking the in situ temperature (± 0.1°C) and light regimes (115 µmol photons m^{-2} s^{-1} in a 12h:12 h light:dark photoperiod for the 0 m samples and in darkness for the 550 m samples), so that the possible role of photoheterotrophs in the processing of surface DOM was included. Removal of heterotrophic prokaryotic cells by filtration was minor (83% ± 7% SE of the initial abundance was retrieved in the water used for the incubations) and mean cell size was virtually unaffected (2.6% ± 1.0% smaller biovolume than in the unfiltered water). However, filtration eliminated most *Synechococcus* and *Prochlorococcus* cyanobacteria as well as virtually all the larger protistan grazers of heterotrophic prokaryotes, since the mean abundance of heterotrophic nanoflagellates in the GF/C filtrate was only 1.5% (E.I. Sabbagh, pers. comm.). We are therefore confident that no extra sources of DOM were included in our experiments. Subsamples were taken twice per day on the first 2 days, then daily until day 6 and finally at day 8. DOC and FDOM subsamples from the incubations were gravity-filtered through pre-rinsed 0.2 Millipore polycarbonate filters. We will occasionally use the letters S and M to refer to the incubations made with water from the surface (0 m) and the Mesopelagic layer (550 m), respectively, followed by D or N to refer to the period of sampling (Day or Night): SD, SN, MD, MN.

2.3. DOC analysis

Samples for DOC were acidified with H_3PO_4 and kept in the dark at 4°C until analysis by high temperature catalytic oxidation at the laboratory. All glass material used was acid-cleaned and burned (450°C, 4.5 h). Consensus reference material of deep sea carbon (42–45 µmol C L^{-1} and 31-33 µmol N L^{-1}) and low carbon water (1-2 µmol C L^{-1}), provided by D. A. Hansell and W. Chen (Univ. of Miami) was used to monitor the accuracy of our DOC concentration measurements. The analytical error of DOC concentration was 1.4 µmol L^{-1}.

2.4. DOM fluorescence measurements and PARAFAC modeling

FDOM samples were stored at 4°C before being analyzed (within 2 days after the completion of the cruise and incubation sample collection). UV-VIS fluorescence spectroscopy was measured using a HORIBA Jobin Yvon AquaLog spectrofluorometer with a 1 cm path length quartz cuvette. Three dimensional fluorescence excitation emission matrices (EEMs) were recorded by scanning with an excitation wavelength range of 240-600 nm and an emission one of 250-600 nm, both at 3 nm increments and integrating at 8 seconds. To correct and calibrate the fluorescence spectra, we followed the post-processing steps of Murphy et al. (2010), in which Raman-normalized Milli-Q blanks were subtracted to remove the Raman scattering signal. All fluorescence spectra were Raman area (RA) normalized by subtracting daily blanks that were performed using Ultra-Pure Milli-Q sealed water (Certified Reference, Starna Cells). Inner-filter correction (IFC) was also applied according to McKnight et al. (2001). MATLAB (version R2015b) was used for the RA normalization, blank subtraction, IFC and generation of EEMs. The EEMs obtained were subjected to PARAFAC modeling using drEEM Toolbox (Murphy et al., 2013). Before the analysis, Rayleigh scatter bands were trimmed [first order at each wavelength pair where Ex = Em ± bandwidth; second order at each wavelength pair where Em = 2 Ex ± (2 × bandwidth)]. No outliers were identified and the model was validated using half split validation and random initialization (Stedmon and Bro, 2008).

The data array consisted of 165 samples (81 from 7 vertical profiles and 84 from the experimental incubations) that were split into two random halves. The nested PARAFAC algorithm was then applied stepwise to both data arrays for 2–7 components. 10 iterations and a convergence criterion of 1e-6 were used for each model. The spectral properties of the components derived from each half were compared and found to be congruent according to the Tucker Coefficient described in Lorenzo-Seva and Ten Berge (2006) for a 4-component model. The 4 components of the validated model are: peak C1 at Ex/Em 240(325)/407 nm, peak C2 at Ex/Em 258(390)/492 nm, peak C3 at Ex/Em 240/337 and peak C4 at Ex/Em 276/312 nm. C1 corresponds to peak M (Coble, 2007) and is comparable to component 2 identified by Català et al. (2015). C2 represents a combination of peaks A and C (Coble, 2007) and is comparable to component 1 in Catalá et al. (2015). C3 corresponds to peak T (Coble, 2007), attributed to tryptophane, and is comparable to component 3 in Catalá et al. (2015). C4 corresponds to peak

B (Coble, 2007), attributed to tyrosine, and is comparable to component 4 in Catalá et al. (2015). The maximum fluorescence (Fmax) is reported in Raman units (RU).

2.5. Heterotrophic prokaryotes abundance and biomass

Triplicate samples (1.8 mL) for estimating the abundance of heterotrophic bacteria and archaea (no distinction between the two domains of prokaryotes was possible) in situ and in the experimental incubations were fixed with 1% paraformaldehyde and 0.05% glutaraldehyde, deep frozen in liquid nitrogen and stored at -80°C until analysis. Once thawed, 400 µL aliquots were stained with SYBR-Green, run in a BD FACSCanto II flow cytometer for estimating the abundance of low (LNA) and high (HNA) nucleic acid content cells as detailed in Gasol and Morán (2015). The few cyanobacteria present were easily distinguished in the surface samples due to their autofluorescence red signal because of the presence of chlorophyll *a*. Absolute abundances were estimated based on time and the actual flow rates, which were calibrated daily using the gravimetric method. The right angle light scatter or side scatter (SSC) signal relative to the value of 1 µm fluorescent latex beads added to each sample was used to estimate the cell diameter according to Calvo-Díaz and Morán (2006). LNA and HNA cell numbers were summed to estimate the total abundance and their specific cell sizes averaged to obtain the mean cell size of the heterotrophic prokaryote community at both depths and different times. Assuming spherical shape, the mean cell size (biovolume in μm^3) was converted into cellular carbon content following Gundersen et al. (2001). Heterotrophic prokaryotes biomass was then calculated as the product of cell abundance and mean cellular carbon content.

2.6. Growth rate estimates

In situ specific growth rates of the heterotrophic prokaryote assemblage at the surface and at the mesopelagic layer were estimated from changes in biomass (µg C L^{-1}) resulting from changes in abundance and mean cell size over 24 h**.** Specific growth rates (µ, in units h^{-1}) were calculated for each sampling point as:

$$\mu = \ln (N_1/N_0) / \Delta t \quad (1)$$

where N_1 is the final biomass, N_0 is the initial biomass and Δt is the time interval (2 h). In order to obtain the diel trend for each layer, we fitted a loess regression model to the hourly estimates. We then modeled the overall daily growth rate using the size distribution of the organisms estimated by flow cytometry, instead of the changes in biomass, with the R package ssPopModel (Ribalet et al., 2015). This routine includes a size-structured matrix population model originally developed by Sosik et al. (2003) and is independent of the cell abundance. The matrix population model assumption is that changes in size distribution are only related to growth and division of the cells. We applied this function to heterotrophic prokaryotic cells without including light measurements as usually done with cyanobacteria (Hunter-Cevera et al., 2014).

Specific growth rates in the incubations were calculated individually for each experimental bottle as the slope of the ln-transformed total abundance vs. time for the linear response period, equivalent to the phase of exponential growth (usually lasting between 2 and 3 days).

2.7. Prokaryotic growth efficiency

Prokaryote heterotrophic production (PHP) in the midnight and midday incubations was estimated as the rate of increase in bacterial biomass during the exponential phase of growth. Prokaryotic carbon demand (PCD, i.e. the sum of heterotrophic prokaryotes production and respiration) was approached by the consumption rate of DOC during the same period. Prokaryotic growth efficiency (PGE) was therefore calculated as the ratio of PHP to PCD.

2.8. Statistical analyses

Model I or ordinary least squares (OLS) linear regressions for estimating specific growth rates were done separately for each replicate, using a common period for each experiment, in order to better account for bottle-specific differences since repeated samplings were dependent on initial values. Differences between treatments and/or depths were assessed with

t-tests and one way ANOVAs followed by Fisher least significance (LSD) post-hoc tests. General relationships between variables were represented by Pearson's correlation coefficients. Statistical analyses were done with JMP and STATISTICA software packages.

3. RESULTS

3.1. Environmental variability of DOC and heterotrophic prokaryotes

The oceanographic characteristics of the study site are shown in Calleja et al. (2019) for the first CTD cast conducted at noon on March 6th 2016 and were closer to the spring average profile than to the winter one (Al-Otaibi et al., 2020), with a mean depth of the upper mixed layer of 36 m (± 3 SD). As previously shown (García et al. 2018), the physico-chemical characteristics other than DOM remained pretty stable during the 24 h occupation of the station, showing no apparent disturbances due to currents or internal waves. For instance, the thermocline depth (estimated as the 24°C isotherm) barely changed (89-93 m) in the 13 profiles. Similarly, the nutricline depth (i.e. the depth where nitrate concentrations reached 1 µmol L^{-1}) was very stable throughout the sampled period (88 ± 9 m). The complete diel vertical migration of the mesopelagic fishes present can be clearly seen in the echogram of **Fig. 1**, with the deeper, more intense DSL (dominated by *Benthosema pterotum*) occupying the depths between ca. 520 and 630 m during daytime. **Fig. 2** shows the diel variability of mean DOC concentrations, HP biomass and cell size at the station's upper 25 m and the mesopelagic layer comprised between 450 and 600 m depth, in order to illustrate that the behaviour of these variables at 0 and 550 m was representative of the upper mixed layer and the DSL, respectively. Mean DOC values were more than 50% higher at 0 than at 550 m (71.0 ± 4.0 SD vs. 45.6 ± 3.6 µmol C L^{-1}, respectively). However, both depths showed similar dynamics, with relative maxima of DOC at noon and also at midnight at the surface (**Fig. 2A)** and a higher variability at the mesopelagic depth (CV 8.1% vs. 5.7%). Given the observed variability, we attempted to calculate hourly rates of apparent DOC production and consumption for the periods of highest increase and decrease, respectively. At the surface, the highest DOC production and consumption took place before and after midnight, while both processes occurred around noon

(production from 8 am to 12 pm and consumption from 12 pm to 4 pm) at 550 m (**Fig. 2A**). The estimated rates were slightly higher in shallow waters: apparent production of 2.6 µmol C L^{-1} h^{-1} and consumption of 1.7 µmol C L^{-1} h^{-1} compared with 2.2 and 1.8 µmol C L^{-1} h^{-1}, respectively, at the DSL depth. Regarding the fluorescent DOM fraction, the protein (Tyrosine)-like component C4 was on average one order of magnitude higher at the surface than at 550 m, although it showed more variability at depth (**Table S1**).

The abundance of HP at the surface (mean 4.31 ± 0.61 SD x 10^5 cells mL^{-1}) was also one order of magnitude higher than at 550 m (mean 9.43 ± 1.42 x 10^4 cells mL^{-1}), but varied similarly with no clear diel patterns. Although their size was 20% ± 7% larger in the mesopelagic (mean values of 0.033 ± 0.002 and 0.028 ± 0.002 µm^3 at 550 and 0 m, respectively, **Fig. 2C**), the corresponding biomass was driven mostly by changes in abundance, averaging 1.91 ± 0.32 µg C L^{-1} at the surface and 0.50 ± 0.08 µg C L^{-1} at 550 m. However, HP biomass was equally variable at both depths (CV 16.8%). **Fig. 2B** shows the biomass values for the upper and deeper layers in µmol C L^{-1} for comparison with DOC concentrations (**Fig. 2A**). The specific growth rates of heterotrophic prokaryotes estimated from in situ biomass changes varied cyclically over the 24 h, especially at the surface, where two maxima were found (at 20:00 and 4:00), while the maximum at 550 m was observed at 16:00 (**Fig. S2**). Daily values based on changes in HP cell size were 0.15 d^{-1} at 0 m and 0.10 d^{-1} at 550 m.

3.2. Experimental incubations of surface and deep samples

With initial concentrations similar to ambient values (**Fig. 2A**), DOC was consumed in the first 2-3 days in the predator-free experiments (**Fig. 3**), albeit at different daily rates (**Table 1**), followed by net production after day 4, especially in the Surface incubations. The cause for this change in dynamics was likely due to food web processes (e.g., viruses were not removed by filtration), since it was accompanied by a steady decrease in heterotrophic prokaryotes biomass (**Fig. 3A, B**). We therefore restricted our analysis to the first periods showing consistent DOC decreases and HP biomass increases. Minimum and maximum consumption rates were 0.32 and 2.69 µmol C L^{-1} d^{-1}, found in the Mesopelagic and Surface Night experiments, respectively (MN and SN). Values in the other two experiments carried out with noon samples were below 1

µmol C L^{-1} d^{-1} (0.47 and 0.95 µmol C L^{-1} d^{-1}, respectively in MD and SD). The initial fluorescence intensity values of the component C4 in the experiments was higher but reflected the values measured concurrently in the water column (paired *t*-test, p>0.05, n=4). C4 showed a very consistent consumption pattern regardless of the layer and treatment. Heterotrophic prokaryotes in the Surface incubations consumed in 4 days 40 and 50% of the initial values during Night and Day respectively, while bacteria inhabiting deep waters consumed almost all of it (95-100 %) within the same time frame regardless of the sampling time (**Fig. 4**). Hereinafter we consider changes in C4 as representative of labile DOM dynamics. Day and night C4 consumption patterns did not show any significant differences within the same layer but they displayed significantly higher consumption rates in the Mesopelagic layer (ANOVA, p=0.004, post-hoc Fisher LSD test, **Figure 4** and **Table S1**).

Heterotrophic prokaryotes responses in the incubation experiments differed between depths and sampling times (**Fig. 3**). Consistent differences were found between the specific growth rates at both depths (**Table 1**), with µ being double in the Surface than in the Mesopelagic experiments. Within each layer, the Day µ values tended also to be higher than the Night ones (t-tests, p=0.020 and p=0.060 at the Surface and Mesopelagic experiment, respectively, n=6). HNA cells always grew faster than their LNA counterparts resulting in increases in their relative contribution from 43-55% to 55-62%, more noticeable in the MD experiment. The mean size of the cells also increased substantially in the Mesopelagic experiments, from 0.027 to 0.060 µm^3 in the MD incubation and from 0.028 to 0.047 µm^3 in the MN one, while changes in cell size were much smaller in the Surface experiments, and virtually the same in both periods: from 0.026 to 0.037 µm^3 (SD) and from 0.025 to 0.035 µm^3 (SN) (**Fig. S2**). Consequently, cell size played an important role in the increase in biomass, especially in both Mesopelagic experiments (**Fig. 3C, D**). The biomass production rates of heterotrophic prokaryotes for the same periods of DOC consumption ranged 4-fold, from 0.010 to 0.047 µmol C L^{-1} d^{-1}, mirroring the changes in the latter variable (**Table 1**). The rates of heterotrophic prokaryotes biomass production and DOC consumption were used for estimating prokaryotic growth efficiencies (PGE) in the four experimental incubations**.** PGE was uniformly below 5%, ranging from 1.8% (SN) to 4.2% (both SD and MD, **Table 1**). Following the pattern of in situ

values, maximum HP biomass measured in the incubations was higher in the Surface than in the Mesopelagic experiments (**Fig. 3**, **Table 1**), although the increase ratios (i.e. the ratio of maximum to initial biomass, **Table 1**) were significantly higher in the Mesopelagic experiments with all data pooled (t-test, p=0.048 , n=12).

4. DISCUSSION

There is consensus that marine biota biomass and activity peak in the upper layers and decrease exponentially with depth, following the strong vertical gradients in physico-chemical properties (Arístegui et al., 2009). Heterotrophic prokaryotes inhabiting the Red Sea seem to challenge this view. Together with diel variations of standing stocks (García et al., 2018, this study), night- and day-initiated incubations of predator-free ambient assemblages with the DOM pool available at the time of sampling yielded surprising similarities in epipelagic and mesopelagic waters. The diel variability in heterotrophic prokaryotes cell size showed similar patterns at the surface and the mesopelagic layer (**Fig. 2C**), yielding low but comparable in situ specific growth rate estimates at both target depths (0.10-0.15 d^{-1}) using a size-structured matrix population model (**Fig. S2**, Sosik et al., 2003; Ribalet et al., 2015). However, it must be noted that although the 550 m depth specific growth rate was lower than the surface one in this study, the already large prokaryotes inhabiting the mesopelagic layer were able to grow much bigger in the absence of protistan grazers (**Fig. S1**), confirming the results of a previous study conducted at the same site (Calleja et al., 2018).

Diel cycles in biogeochemical properties and plankton biomass and activity in the upper ocean layers are reasonably well known, following diurnal changes in photosynthesis and food web processes (Gasol et al., 1998; Ruiz-González et al., 2012). Diel patterns are not easy to discern in a single 24 h in situ sampling with all the components of the microbial food web present, but **Fig. 2** shows that the variability in DOC and heterotrophic prokaryotes stocks in the mesopelagic was comparable to that found at the surface, an arguably much more dynamic environment. Consequently, no clear patterns were observed for in situ heterotrophic prokaryotes abundance or biomass, probably due to the strong coupling between growth and mortality due to protistan grazing (Calbet et al., 2015; Silva et al., 2019) and/or viral lysis in the

Red Sea (Sabbagh et al., 2020), and in tropical waters in general (Morán et al., 2017). However, likewise early observations in the Caribbean (Johnson et al., 1981) recently confirmed for this site by García et al. (2018), DOM concentrations displayed a coherent diel pattern suggesting different timing of production and consumption (**Fig. 2A**). Although part of the apparent in situ consumption of DOC at the surface could indeed have been caused by photobleaching, this process is mostly caused by UV radiation, which was prevented in our subsequent laboratory incubations. In any case, photobleaching is more likely to have affected the FDOM components rather than the bulk DOC concentration (Mopper et al. 2014).

The exclusion of protistan grazers in the experiments decoupled the microbial food web from trophic interactions other than the processing of DOM by heterotrophic prokaryotes, although we cannot discard that viruses might have had a role. It can be argued that any daily input should be consumed in one day but, yet fast, DOC and FDOM component C4 consumption occasionally extended up to 48 or 72 h. As in previous experiments (Calleja et al., 2018), DOC consistently decreased in the first 2 to 3 days in both Surface and Mesopelagic samples experiments, ranging from 0.7 to 6.1 µmol L^{-1} (**Fig. 3A, B**). Indeed, the strong apparent uptake of surface DOC in situ during nighttime coincided with the highest DOC consumption experimental result, pointing to its labile nature, although the buildup of HP biomass was similar in both SD and SN experiments, resulting in lower specific growth rates and PGE values in the Night (**Table 1**).

Labile DOC incorporation does not automatically inform us of its subsequent partitioning between metabolism (respiration) and growth (biomass production), as shown by Condon et al. (2011) for DOM originated by jellyfish blooms. Since the alternation between light and dark periods within the incubator used for Surface seawater was common for SD and SN experiments, if photoheterotrophy (Béjà et al., 2000; Ruiz-González et al. 2013) afffected DOM dynamics, it should have been equally apparent in both Night and Day incubations, which were initiated with ony 12 h difference (**Fig. 1**). We therefore ruled out photoheterotrophic processes explaining the differences observed after 8 days of incubation. Rather, the quality of labile DOM at midday (including recent photosynthate) was probably higher than at midnight, perhaps with a greater contribution of DOM coming from sloppy feeding (Nagata, 2000),

causing the significantly higher, almost double, μ value in the SD experiment (**Table 1**). That the quality of labile DOC at noon could have been higher was supported by a faster increase in bacterial cell size (**Fig. S1B**) and the contribution of HNA cells, which increased by 35% in SD compared with 15% in SN. The decrease in the protein-like C4 component was also more sustained in the SD experiment compared to SN after 4 days (13.2% vs. 5.3% was consumed daily during that period, **Fig. 4**) although the rates were virtually the same in the initial periods (2.75 and 2.25 days, respectively, **Table S1**).

Changes in mesopelagic DOC concentrations and lability at diel (García et al., 2018, this study) and seasonal scales (Calleja et al., 2019) in the central Red Sea support the recent claim that the diverse pool of DOM in the deep ocean fluctuates at timescales much shorter than previously thought (Follett et al., 2014). Since the conditions at the study site were hypoxic in most of the mesopelagic realm (Calleja et al., 2019), the low in situ oxygen concentrations in the Mesopelagic water samples, consistent from 200 m downwards (0.69 ± 0.03 mg L^{-1}) might have been supplemented by pre-filtration and sampling from the experimental bottles. Although we did not control for this potential artefact, the same protocol was followed for the MN and MD experiments. Therefore, the consistently higher values of DOM consumption, prokaryotic cell size, growth rates and efficiency in the Day compared with the Night incubation of DSL water strongly support that the presence of fish indeed had a major impact on the microbial community. Contrary to other sites, virtually no fishes remain at the DSL depth during the night in the central Red Sea (Klevjer et al., 2012), likely strengthening the differences between the Night and Day incubations of the Mesopelagic samples.

Surface HP specific growth rate in the Day experiment was nevertheless notably higher than the 0.08 d^{-1} measured in a previous study carried out in November 2015 at the same location (Calleja et al., 2018). The discrepancy cannot be explained by total DOC or chlorophyll *a* surface concentrations, but could instead be related to the availability of labile DOM compounds since C4 concentrations were 61% higher in March than in November (M. L. Calleja, pers. comm.). At a shallower, nearby site characterized by higher total and labile DOC concentrations, specific growth rates were still considerably higher, ranging from 0.79 to 1.75 d^{-1} (Silva et al., 2019).

Changes in in situ DOC concentration in surface and mesopelagic waters over 24 hours indicated no net accumulation (**Fig. 2A**). This is the expected result in oligotrophic regions at the short time scale of one day (Johnson et al., 1981; Wright, 1984). However, although the mean daily rates of apparent DOC production/consumption were ca. 10% higher at the surface than in the DSL, the estimated turnover of labile DOC, considering the respective measured DOC variability and mean concentrations, was 17% d^{-1} at 550 m and 12% d^{-1} at 0 m. This finding conflicts with the contention that DOM is largely of refractory nature within the mesopelagic waters of the global ocean (Jiao et al., 2010). The role of vertically migrating animals, zooplankton and fishes, as vectors of organic matter to deep layers complementary to the biological pump (Herndl and Reinthaler, 2013) has been recently recognized (Bianchi et al., 2013a,b; Isla et al., 2015). In this regard, work at the study site has suggested DVM fishes as a transport mechanism supplying labile DOM that does not accumulate but fuels heterotrohic bacterial activity in mesopelagic waters (Calleja et al., 2018). Here we tested this hypothesis by further examining the fluorescence properties of DOM and its transformation by heterotrophic prokaryotes in experimental incubations of samples taken with and without the fishes present. FDOM are useful tracers for biogeochemical processes in the dark ocean (Nelson and Siegel, 2013; Catalá et al., 2015). Fluorescence intensity of the two aminoacid-like fluorophores C3 and C4 decreased with depth (data not shown), indicating that these fluorophores were mainly produced autochthonously in surface waters. Both phytoplankton and bacteria are sources of tryptophan and tyrosine (Determann et al., 1998), while Urban-Rich et al. (2006) have reported that grazing and excretion by zooplankton can also release material with amino acid-like fluorescence signals. Our results strongly suggest that DVM fishes can also provide C4 in the mesopelagic realm.

Contrary to the epipelagic zone, very few studies on the diel variability of DOM-heterotrophic prokaryotes interactions are available for deep waters (García et al., 2018; Carlucci et al., 1986). Gasol et al. (2009) suggested that mesopelagic prokaryotes in the subtropical NE Atlantic were as active as the epipelagic counterparts. We demonstrate here not only that heterotrophic prokaryotes specific growth rates at 550 m were of the same order of magnitude than in surface waters, clearly challenging the most accepted view (Arístegui et al.,

2009; Baltar et al. 2010), but that those rates were almost double at noon conditions, when the mesopelagic fishes were present at the DSL, than at midnight, when the entire population was closer to the surface (Klevjer et al., 2012) and no DSL could be seen (**Fig. 1**)**.** Fishes present in the upper layers at night do not contribute significantly to the DOM pool; rather, at the surface it is phytoplankton primary production driving the diel dynamics. From **Fig. 1** it is clear that the fishes were absent at midnight in the entire mesopelagic zone but their presence at 550 m had been established for ca. 4 h when the noon sampling took place. Specific growth rates were nevertheless lower than in the previous study (0.24 d^{-1}, Calleja et al., 2018). Although seasonality of C4 in the DSL was less marked than at the surface, November 2015 was characterized by 82% higher C4 concentrations than in March 2016 (M.L. Calleja, pers. comm.). Altogether, these results point out to a major role of protein-like substances in determining the specific growth rates of heterotrophic prokaryotes throughout the water column, as recently found for nearby shallow waters in a seasonal study (Silva et al., 2019). C4 fluctuated widely in the 24 h monitoring at 550 m depth (**Table S1**) and was also actively consumed in all our incubations, thus revealing a clearly labile nature. C4 was consumed faster in the Mesopelagic experiments, at 42.1% and 25.8% d^{-1} in MD and MN, respectively (**Fig. 4, Table S1**), than in the Surface ones (ca. 13% d^{-1} in both SD and SN). A similar relative consumption of protein-like FDOM (12% d^{-1}), mostly occurring during the first 5 days, was measured by Yamashita and Tanoue (2004) in experiments conducted with marine surface waters. Our explanation is that fishes released DOM directly or it leaked from particles associated to the fish presence (e.g. fecal pellets). That DOM could have been delivered by sinking particles (Smith et al., 1992) not related to vertical migration would not explain the difference between the MD and MN experiments. Due to logistic constraints, our experimental design did not allow for more mesopelagic layers to be compared with the depth occupied by fishes during daytime. However, a previous study demonstrated significant differences between the biomass production of heterotrophic prokaryotes between 275 and 550 m, higher for the latter (Calleja et al., 2018).

Cell size has been used as an indicator of heterotrophic prokaryotes activity (Gasol et al., 1995). While in the Surface experiment growing HP cells were only slightly larger than at time 0

(11% larger size for both the SD and SN experiments), the cell size increase in the Mesopelagic experiment was dramatic, especially in the Day incubations (118% larger in MD vs. 68% in MN, **Fig. S2**). The contribution of bigger cells to the observed increase in HP biomass is not at all minor: had we used, as in many studies, a fixed cellular carbon content of 4 fg C $cell^{-1}$ (corresponding to the initial mean cell size of 0.027 μm^3 for the two depths and periods, **Fig. 2C**), maximum HP biomass in **Table 1** would have become 2.10 (SD), 2.32, (SN), 0.43 (MD) and 0.39 (MN) µg C L^{-1}, i.e. between 42 and 54% lower than the actual values for the mesopelagic prokaryotes. We can safely conclude that the presence of fishes in the DSL of the mesopelagic zone during daytime resulted in significantly higher growth rates of markedly larger cells. As a consequence, changes in abundance were exacerbated when considering biomass units. The maximum biomass of heterotrophic prokaryotes that could be sustained by extant DOM concentrations was significantly higher than the initial value in both Mesopelagic experiments (**Table 1**). Altogether, these results point out to substantial inputs of labile DOM during daytime at the mesopelagic fish layer that are rapidly mobilized by large bacterial taxa. The archaeon *Nitrosopulimus maritimus,* which makes up much of the heterotrophic prokaryoplankton biomass at these depths (Ngugi et al., 2012), were apparently not the main responders to these DOM hotspots, since their contribution to total numbers at the end of a similar incubation dropped from 50% to 3% (Calleja et al., 2018). The typical size of these Thaumarchaeota is small (Konneke et al., 2005), so it is unlikely that they were the dominant groups growing in our Mesopelagic incubations after 2 days (**Fig. S2C, D**). Besides excreting ammonia that boosts its oxidation by Thaumarchaeota (formely known as Chrenarchaeota, Bianchi et al., 2014), mesopelagic fish thus seem capable to fuel the metabolism of large, copiotrophic bacteria.

Prokaryotic growth efficiencies are typically low in open ocean, oligotrophic environments (del Giorgio and Cole, 1998; Reinthaler et al. 2006). Most of these measurements refer to the epipelagic zone, where photosynthesis takes place. Here we provide more information from deeper layers, where export processes are more important. The recently reported low PGE values at this Red Sea site (1.6-3.4%,Calleja et al., 2018) are confirmed by this new study, while higher values (2.5-12.8%) were recorded in a shallow, richer bay located a few km south (Silva et al., 2019). Few studies have estimated the vertical variability in PGE values,

but those that have usually depict lower values with depth (Reinthaler et al., 2006; Lemée et al., 2002), related to the increased presence of refractory DOM compounds (Jiao et al., 2010) or to the higher dilution of the labile ones (Arrieta et al., 2015). Notably, the estimated growth efficiency of heterotrophic prokaryotes in our Day experiments was exactly the same in Surface and Mesopelagic water (4.2%), which can only be explained by the existence of labile DOC of similar quality within both layers, likely resulting from photosynthesis at the surface and fish-mediated export in the mesopelagic layer. PGE in the mesopelagic fish layer was significantly higher than at shallower depths in the experiment conducted at noon in November 2015 (Calleja et al., 2018). However, when averaging our new two estimates, the mean PGE value at 550 m (3.6%) was still 22% higher than at the surface, strongly supporting the presence of high quality DOM hotspots (Calleja et al., 2018) in the DSL.

5. CONCLUSIONS

This study builds on the previously demonstrated relatively high growth of mesopelagic heterotrophic prokaryotes (Calleja et al., 2018) by comparing the outcome of deep samples incubations taken only 12 hours apart, at midnight and noon, with in situ observations during 24 hours. We show that the Red Sea mesopelagic zone is not a permanently impoverished environment but seemingly subject to daily inputs of labile DOM compounds similarly to the fresh photosynthate being released in the epipelagic layers. This novel process, plausibly driven by mesopelagic fishes, which complements other recently discovered sources of deep organic carbon (Herndl and Reinthaler, 2013; Dall'Olmo et al., 2016; Giering et al., 2014; Boeuf et al., 2019) seems to have been overlooked due to the tight coupling between the components of microbial food webs (Pernthaler, 2005). Although challenging, additional investigations ideally including healthy DVM mesopelagic fishes and the microbial plankton community would directly establish the cause-effect link we suggest here. If vertically migrating fishes are able to fuel an active and taxonomically distinct (T.M. Huete-Stauffer et al., pers. comm.) community of heterotrophic prokaryotes in the mesopelagic layer of the Red Sea, we might expect this rapid processing of labile DOM inputs to be widespread. The mesopelagic Red Sea has an unusually high temperature, therefore the effect of colder conditions on fish DOM-microbial interactions

remains to be explored. The implications for global biogeochemical cycling would also vary depending on the actual biomass of mesopelagic fishes and the fraction performing DVM (Klevjer et al., 2016), yet its impact may increase as deep waters warm up (Luna et al., 2012). That these small fishes seem able to sustain the microbial communities inhabiting the twilight zone also may help reconcile current discrepancies between carbon pools and fluxes in the global ocean.

ACKNOWLEDGMENTS

We are greatly indebted to the crew of RV Thuwal and the rest of the personnel from the Coastal and Marine Resources (CMOR) Core Lab at KAUST for their assistance during field work. Besides participating in the sample collection M. Vieg as helped us with the rest of the work in the Red Sea Research Center (RSRC) lab. We are also grateful to past members of the Microbial Oceanography and Biogeochemistry lab at the RSRC.

REFERENCES

Al-Mutairi H, Landry MR. 2001. Active export of carbon and nitrogen at Station ALOHA by diel migrant zooplankton. Deep-Sea Res. II 48, 2083-2103.

Alongi DM, Mukhopadhyay SK. 2015. Contribution of mangroves to coastal carbon cycling in low latitude seas. Agr. Forest Meteorol. 213, 266-272.

Al-Otaibi N, Huete-Stauffer TM, Calleja ML, Irigoien X, Morán XAG**.** 2020. Seasonal variability and vertical distribution of autotrophic and heterotrophic picoplankton in the Central Red Sea. PeerJ 8, e8612.

Arístegui J, Gasol JM, Duarte CM, Herndl GJ. 2009. Microbial oceanography of the dark ocean's pelagic realm. Limnol. Oceanogr. 54, 1501-1529.

Arrieta JM, Mayol E, Hansman RL, Herndl GJ, Dittmar T, Duarte CM. 2015. Dilution limits dissolved organic carbon utilization in the deep ocean. Science 348, 331-333.

Baines SB, Pace ML. 1991. The production of dissolved organic matter by phytoplankton and its importance to bacteria: Patterns across marine and freshwater systems. Limnol. Oceanogr. 36, 1078-1090.

Baltar F, Arístegui J, Gasol JM, Herndl GJ. 2010. Prokaryotic carbon utilization in the dark ocean: growth efficiency, leucine-to-carbon conversion factors, and their relation. Aquat. Microb. Ecol. 60, 227-232.

Bao HY, Niggemann J, Luo L, Dittmar T, Kao SJ. 2018. Molecular composition and origin of water-soluble organic matter in marine aerosols in the Pacific off China. Atmos. Environ. 191, 27-35.

Béjà O, Aravind L, Koonin EV, Suzuki MT, Hadd A, Nguyen LP, et al. 2000. Bacterial rhodopsin: evidence for a new type of phototrophy in the sea. Science 289, 1902-1906.

Bianchi D, Babbin AR, Galbraith ED. 2014. Enhancement of anammox by the excretion of diel vertical migrators. Proc. Natl. Acad. Sci. USA 111, 15653-15658.

Bianchi D, Galbraith ED, Carozza DA, Mislan KAS, Stock CA. 2013a. Intensification of open-ocean oxygen depletion by vertically migrating animals. Nat. Geosci. 6, 545-548.

Bianchi D, Stock C, Galbraith ED, Sarmiento JL. 2013b. Diel vertical migration: Ecological controls and impacts on the biological pump in a one-dimensional ocean model. Global Biogeochem. Cycles 27, 478-491.

Boeuf D, Edwards BR, Eppley JM, Hu SK, Poff KE, Romano AE, et al. 2019. Biological composition and microbial dynamics of sinking particulate organic matter at abyssal depths in the oligotrophic open ocean. Proc. Natl. Acad. Sci. USA 16, 11824-11832.

Bouvier T, del Giorgio PA, Gasol JM. 2007. A comparative study of the cytometric characteristics of High and Low nucleic-acid bacterioplankton cells from different aquatic ecosystems. Environ. Microbiol. 9, 2050-2066.

Calbet A, Agersted MD, Kaartvedt S, Mohl M, Moller EF, Enghoff-Poulsen S, et al. 2015. Heterogeneous distribution of plankton within the mixed layer and its implications for bloom formation in tropical seas. Sci. Rep. 5, 11240.

Calleja ML, Al-Otaibi N, Morán XAG. 2019. Dissolved organic carbon contribution to oxygen respiration in the central Red Sea. Sci. Rep. 9, 4690.

Calleja ML, Ansari MI, Røstad A, Silva L, Kaartvedt S, Irigoien X, et al. 2018. The mesopelagic scattering layer: A hotspot for heterotrophic prokaryotes in the Red Sea twilight zone. Front. Mar. Sci. 5, 259.

Calvo-Díaz A, Morán XAG. 2006. Seasonal dynamics of picoplankton in shelf waters of the southern Bay of Biscay. Aquat. Microb. Ecol. 42, 159-174.

Carlson CA, Ducklow HW, Michaels AF. 1994. Annual flux of dissolved organic carbon from the euphotic zone in the northwestern Sargasso Sea. Nature 371, 405-408.

Carlucci AF, Craven DB, Robertson KJ, Henrichs SM. 1986. Microheterotrophic Utilization of Dissolved Free Amino-Acids in Depth Profiles of Southern-California Borderland Basin Waters. Oceanol. Acta 9, 89-96.

Catalá TS, Reche I, Fuentes-Lema A, Romera-Castillo C, Nieto-Cid M, Ortega-Retuerta E, et al. 2015. Turnover time of fluorescent dissolved organic matter in the dark global ocean. Nat. Commun. 6, 5986.

Coble PG. 2007. Marine optical biogeochemistry: The chemistry of ocean color. Chem. Rev. 107, 402-418.

Condon RH, Steinberg DK, del Giorgio PA, Bouvier TC, Bronk DA, Graham WM, et al. 2011. Jellyfish blooms result in a major microbial respiratory sink of carbon in marine systems. Proc. Natl. Acad. Sci. USA 108, 10225-10230.

Dall'Olmo G, Dingle J, Polimene L, Brewin RJW, Claustre H. 2016. Substantial energy input to the mesopelagic ecosystem from the seasonal mixed-layer pump. Nat. Geosci. 9, 820-823.

del Giorgio PA, Cole JJ. 1998. Bacterial growth efficiency in natural aquatic systems. Ann. Rev. Ecol. Syst. 29, 503-541.

Determann S, Lobbes JM, Reuter R, Rullkotter J. 1998. Ultraviolet fluorescence excitation and emission spectroscopy of marine algae and bacteria. Mar. Chem. 62, 137-156.

Duarte CM, Cebrián J. 1996. The fate of marine autotrophic production. Limnol. Oceanogr. 41, 1758-1766.

Follett CL, Repeta DJ, Rothman DH, Xu L, Santinelli C. 2014. Hidden cycle of dissolved organic carbon in the deep ocean. Proc. Natl. Acad. Sci. USA 2014, 16706-16711.

Fouilland E, Mostajir B. 2010. Revisited phytoplanktonic carbon dependency of heterotrophic bacteria in freshwaters, transitional, coastal and oceanic waters. FEMS Microbiol. Ecol. 73, 419-429.

García FC, Calleja ML, Al Otaibi N, Røstad A, Morán XAG. 2018. Diel dynamics and coupling of heterotrophic prokaryotes and dissolved organic matter in epipelagic and mesopelagic waters of the central Red Sea. Environ. Microbiol. 20, 2990-3000.

Gasol JM, Alonso-Sáez L, Vaqué D, Baltar F, Calleja ML, Duarte CM, et al. 2009. Mesopelagic prokaryotic bulk and single-cell heterotrophic activity and community composition in the NW Africa-Canary Islands coastal-transition zone. Prog. Oceanogr. 83, 189-196.

Gasol JM, del Giorgio PA, Massana R, Duarte CM. 1995. Active versus inactive bacteria: size-dependence in coastal marine plankton community. Mar. Ecol. Prog. Ser. 128, 91-97.

Gasol JM, Doval MD, Pinhassi J, Calderón-Paz JI, Guixa-Boixareu N, Vaqué D, et al. 1998. Diel variations in bacterial heterotrophic activity and growth in the northwestern Mediterranean Sea. Mar. Ecol. Prog. Ser. 164, 107-124.

Gasol JM, Morán XAG. 2015. Flow cytometric determination of microbial abundances and its use to obtain indices of community structure and relative activity. In: McGenity TJ, Timmis KN, Nogales B (eds). Hydrocarbon and Lipid Microbiology Protocols. Springer: Berlin, Germany, pp 159-187.

Gasol JM, Zweifel UL, Peters F, Fuhrman JA, Hagström Å. 1999. Significance of size and nucleic acid content heterogeneity as measured by flow cytometry in natural planktonic bacteria. Appl. Environ. Microbiol. 65, 4475-4483.

Giering SLC, Sanders R, Lampitt RS, Anderson TR, Tamburini C, Boutrif M, et al. 2014. Reconciliation of the carbon budget in the ocean's twilight zone. Nature 507, 480-483

Goldman JC, Dennett MR. 2000. Growth of marine bacteria in batch and continuous culture under carbon and nitrogen limitation. Limnol. Oceanogr., 45: 789-800.

Gundersen K, Orcutt KM, Purdie DM, Michaels AF, Knap AH. 2001. Particulate organic carbon mass distribution at the Bermuda Atlantic Time-series Study (BATS) site. Deep-Sea Res. II 48, 1697-1718.

Henson SA, Sanders R, Madsen E. 2012. Global patterns in efficiency of particulate organic carbon export and transfer to the deep ocean. Global Biogeochem. Cycles 26, GB1028.

Herndl GJ, Reinthaler T. 2013. Microbial control of the dark end of the biological pump. Nat. Geosci. 6, 718-724.

Hunter-Cevera KR, Neubert MG, Solow AR, Olson RJ, Shalapyonok A, Sosik HM. 2014. Diel size distributions reveal seasonal growth dynamics of a coastal phytoplankter. Proc. Natl. Acad. Sci. USA 111, 9852-9857.

Irigoien X, Klevjer TA, Rostad A, Martinez U, Boyra G, Acuña JL, et al. 2014. Large mesopelagic fishes biomass and trophic efficiency in the open ocean. Nat. Commun. 5, 3271.

Isla A, Scharek R, Latasa M. 2015. Zooplankton diel vertical migration and contribution to deep active carbon flux in the NW Mediterranean. Journal of Marine Systems 143, 86-97.

Jiao N, Herndl GJ, Hansell DA, Benner R, Kattner G, Wilhelm SW, et al. 2010. Microbial production of recalcitrant dissolved organic matter: long-term carbon storage in the global ocean. Nat. Rev. Microbiol. 8, 593-599.

Johnson KM, Burney CM, Sieburth JM. 1981. Enigmatic marine ecosystem metabolism measured by direct diel Sigma-CO_2 and O_2 flux in conjunction with DOC release and uptake. Mar. Biol. 65, 49-60.

Klevjer TA, Irigoien X, Rostad A, Fraile-Nuez E, Benitez-Barrios VM, Kaartvedt S. 2016. Large scale patterns in vertical distribution and behaviour of mesopelagic scattering layers. Sci. Rep. 6, 19873.

Klevjer TA, Torres DJ, Kaartvedt S. 2012. Distribution and diel vertical movements of mesopelagic scattering layers in the Red Sea. Mar. Biol. 159, 1833-1841.

Konneke M, Bernhard AE, de la Torre JR, Walker CB, Waterbury JB, Stahl DA. 2005. Isolation of an autotrophic ammonia-oxidizing marine archaeon. Nature 437, 543-546.

Lekunberri I, Lefort T, Romero E, Vázquez-Domínguez E, Romera-Castillo C, Marrasé C, et al. 2010. Effects of a dust deposition event on coastal marine microbial abundance and activity, bacterial community structure and ecosystem function. J. Plankton Res. 32, 381-396.

Lemée R, Rochelle-Newall E, Van Wambeke F, Pizay MD, Rinaldi P, Gattuso JP. 2002. Seasonal variation of bacterial production, respiration and growth efficiency in the open NW Mediterranean Sea. Aquat. Microb. Ecol. 29, 227-237.

Lorenzo-Seva U, Ten Berge JMF. 2006. Tucker's congruence coefficient as a meaningful index of factor similarity. Methodology 2: 57–64.

Luna GM, Bianchelli S, Decembrini F, De Domenico E, Danovaro R, Dell'Anno A. 2012. The dark portion of the Mediterranean Sea is a bioreactor of organic matter cycling. Global Biogeochem. Cycles 26, GB2017.

McKnight DM, Boyer EW, Westerhoff PK, Doran PT, Kulbe T, Andersen DT 2001. Spectrofluorometric characterization of dissolved organic matter for indication of precursor organic material and aromaticity. Limnol. Oceanogr. 46, 38–48.

Mopper K, Kieber DJ, Stubbins A 2014. Marine Photochemistry of Organic Matter: Processes and Impacts. Processes and Impacts, pp. 389-450. In: Hansell D and Carlson C "Biogeochemistry of Marine Dissolved Organic Matter. Second Edition", eds., Academic Press, 712 pp

Morán XAG, Alonso-Sáez L. 2011. Independence of bacteria on phytoplankton? Insufficient support for Fouilland & Mostajir's (2010) suggested new concept. FEMS Microbiol. Ecol. 78, 203-205.

Morán XAG, Ducklow HW, Erickson M. 2011. Single-cell physiological structure and growth rates of heterotrophic bacteria in a temperate estuary (Waquoit Bay, Massachusetts). Limnol. Oceanogr. 56, 37-48.

Morán XAG, Estrada M, Gasol JM, Pedrós-Alió C. 2002. Dissolved primary production and the strength of phytoplankton-bacterioplankton coupling in contrasting marine regions. Microb. Ecol. 44, 217-223.

Morán XAG, Gasol JM, Pernice MC, Mangot JF, Massana R, Lara E, et al. 2017. Temperature regulation of marine heterotrophic prokaryotes increases latitudinally as a breach between bottom-up and top-down controls. Global Change Biol. 23, 3956-3964.

Murphy KR, Butler KD, Spencer RGM, Stedmon CA, Boehme JR, Aiken GR. 2010. Measurement of Dissolved Organic Matter Fluorescence in Aquatic Environments: An Interlaboratory Comparison. Environ. Sci. Technol. 44, 9405-9412.

Murphy KR, Stedmon CA, Graeber D, Bro R. 2013. Fluorescence spectroscopy and multi-way techniques. PARAFAC. Anal. Methods 5: 6557–6566.

Nagata T. 2000. Production mechanisms of dissolved organic matter. In: Kirchman DL (ed). Microbial ecology of the oceans. Wiley-Liss: New York, pp 121-152.

Nelson NB, Siegel DA. 2013. The Global Distribution and Dynamics of Chromophoric Dissolved Organic Matter. Ann. Rev. Mar. Sci. 5, 447-476.

Ngugi DK, Antunes A, Brune A, Stingl U. 2012. Biogeography of pelagic bacterioplankton across an antagonistic temperature-salinity gradient in the Red Sea. Mol. Ecol. 21, 388-405.

Pernthaler J. 2005. Predation on prokaryotes in the water column and its ecological implications. Nat. Rev. Microbiol. 3, 537-546.

Pomeroy LR, Williams PJI, Azam F, Hobbie JE. 2007. The Microbial Loop. Oceanography 20, 28-33.

Ribalet F, Swalwell J, Clayton S, Jiménez V, Sudek S, Lin Y, Johnson ZI, Worden AZ, Armbrust EV 2015. Light-driven synchrony of *Prochlorococcus* growth and mortality in the subtropical Pacific gyre. Proc. Natl. Acad. Sci. USA 112, 8008-8012.

Reinthaler T, van Aken H, Veth C, Arístegui J, Robinson C, Williams PJLB, et al. 2006. Prokaryotic respiration and production in the meso- and bathypelagic realm of the eastern and western North Atlantic basin. Limnol. Oceanogr. 51, 1262-1273.

Robinson C, Steinberg DK, Anderson TR, Arístegui J, Carlson CA, Frost JR, et al. 2010. Mesopelagic zone ecology and biogeochemistry - a synthesis. Deep-Sea Res. II 57, 1504-1518.

Røstad A, Kaartvedt S, Aksnes DL. 2016. Light comfort zones of mesopelagic acoustic scattering layers in two contrasting optical environments. Deep Sea Res. I 113, 1-6.

Ruiz-González C, Lefort T, Massana R, Simó R, Gasol JM. 2012. Diel changes in bulk and single-cell bacterial heterotrophic activity in winter surface waters of the northwestern Mediterranean Sea. Limnol. Oceanogr. 57, 29-42.

Ruiz-González C, Simó R, Sommaruga R, Gasol JM. 2013. Away from darkness: a review on the effects of solar radiation on heterotrophic bacterioplankton activity. Front. Microbiol. 4, 131.

Sabbagh EI, Huete-Stauffer TM, Calleja MLl, Silva L, Viegas M, Morán XAG. 2020. Weekly variations of viruses and heterotrophic nanoflagellates and their potential impact on bacterioplankton in shallow waters of the central Red Sea. FEMS Microbiol. Ecol. 96, fiaa03336.

Schattenhofer M, Wulf J, Kostadinov I, Glockner FO, Zubkov MV, Fuchs BM. 2011. Phylogenetic characterisation of picoplanktonic populations with high and low nucleic acid content in the North Atlantic Ocean. Syst. Appl. Microbiol. 34, 470-475.

Silva L, Calleja ML, Huete-Stauffer TM, Ivetic S, Ansari MI, Viegas M, et al. 2019. Low abundances but high growth rates of heterotrophic bacteria in the coastal Red Sea. Front Microbiol 9, 3244.

Smith DC, Simon M, Alldredge AL, Azam F. 1992. Intense Hydrolytic Enzyme-Activity on Marine Aggregates and Implications for Rapid Particle Dissolution. Nature 359, 139-142.

Sosik HM, Olson RJ, Neubert MG, Shalapyonok A, Solow AR. 2003. Growth rates of coastal phytoplankton from time-series measurements with a submersible flow cytometer. Limnol. Oceanogr. 48, 1756-1765.

Stedmon CA, Bro R. 2008. Characterizing dissolved organic matter fluorescence with parallel factor analysis: a tutorial. Limnol. Oceanogr. Meth. 6, 572-579.

Urban-Rich J, McCarty JT, Fernandez D, Acuña JL. 2006. Larvaceans and copepods excrete fluorescent dissolved organic matter (FDOM). J. Exp. Mar. Biol. Ecol. 332, 96-105.

Vila-Costa M, Gasol JM, Sharma S, Moran MA. 2012. Community analysis of high- and low-nucleic acid-containing bacteria in NW Mediterranean coastal waters using 16S rDNA pyrosequencing. Environ. Microbiol. 14, 1390-1402.

Wang F, Wu Y, Chen Z, Zhang G, Zhang J, Zheng S, Kattner G. 2019. Trophic interactions of mesopelagic fishes in the South China Sea illustrated by stable isotopes and fatty acids. Front. Mar. Sci. 5, 522.

Wright RT. Dynamics of pools of dissolved organic carbon. 1984. In: Hobbie JE, Williams PJlB (eds). Heterotrophic activity in the sea. Plenum Press: New York, pp 121-155.

Yamashita Y, Tanoue E. 2004. In situ production of chromophoric dissolved organic matter in coastal environments. Geophys. Res. Lett. 31, L14302.

Table 1. Mean ± SE values of specific growth rates (μ), DOC consumption rates or prokaryotic carbon demand (PCD, see the text), prokaryotic heterotrophic production rates (PHP) and prokaryotic growth efficiency (PGE) in the surface and mesopelagic layer incubation experiments performed at noon (Day) and midnight (Night). Rates were calculated for each period of exponential growth, also indicated in days. The same period was used for DOC consumption and biomass production rates. Also indicated are the maximum heterotrophic prokaryotes biomass reached within the incubation and the corresponding ratio of maximum to initial biomass (Max:t0 biomass ratio).

Layer	Time	Period (d)	μ (d^{-1})	DOC consumption rate (μmol C L^{-1} d^{-1})	PHP rate (μmol C L^{-1} d^{-1})	PGE (%)	Maximum HP biomass (μg C L^{-1})	Max:t0 HP biomass ratio
Surface	Day	0-1.75	0.34 ± 0.07	1.0 ± 0.5	0.040 ± 0.004	4.2	2.69 ± 0.20	2.30
	Night[a]	0-2.25	0.18 ± 0.02	2.7 ± 1.1	0.047 ± 0.006	1.8	2.85 ± 0.16	1.80
Mesopelagic	Day[a]	0-2.75	0.16 ± 0.01	0.5 ± 0.3	0.020 ± 0.004	4.2	0.94 ± 0.13	3.27
	Night	0-2.25	0.09 ± 0.01	0.3 ± 0.8	0.010 ± 0.001	3.1	0.68 ± 0.02	2.31

[a]Vertically migrating mesopelagic fish present

FIGURE LEGENDS

Fig. 1. Echogram from March 5th to 6th 2016 at the study site showing 2 scattering layers of mesopelagic fish performing diel vertical migration: up to the surface at night and down to deep waters during daytime. Squares indicate the depth and time of water collection for the incubation experiments. Surface and mesopelagic depths are represented in green and blue, respectively, for coherence with subsequent figures. Colour scale indicates backscattering strength (Sv, dB).

Fig. 2. Variability of mean DOC concentration (**A**) and heterotrophic prokaryoplankton biomass (**B**) and cell size (**C**) in two depth ranges of the study site: upper (0-25 m) and mesopelagic occupied by fish during daytime (450-600 m) during the 24 h sampling. Surface and mesopelagic depths are represented in green and blue, respectively. Squares indicate initial values at the onset of the experimental incubations. The gray area represents nightime hours at the date of sampling. Error bars represent the standard error of the mean (average of 0 and 25 m in the upper layer and 450, 550 and 600 m in the mesopelagic one).

Fig. 3. Dynamics of heterotrophic prokaryoplankton biomass (closed symbols) and DOC concentration (open symbols) in the predator-free experimental incubations of samples taken at midnight (**A, C**) and at noon (**B, D**) from the surface and the mesopelagic (550 m depth) layers. Note the different scales for the surface and mesopelagic water experiments. Error bars are standard errors of 3 replicates.

Fig. 4. Dynamics of the concentration of the FDOM protein-like C4 component in the predator-free experimental incubations of samples taken at midnight (**A, C**) and at noon (**B, D**) from the surface and the mesopelagic layers. Error bars are standard errors of 3 replicates.

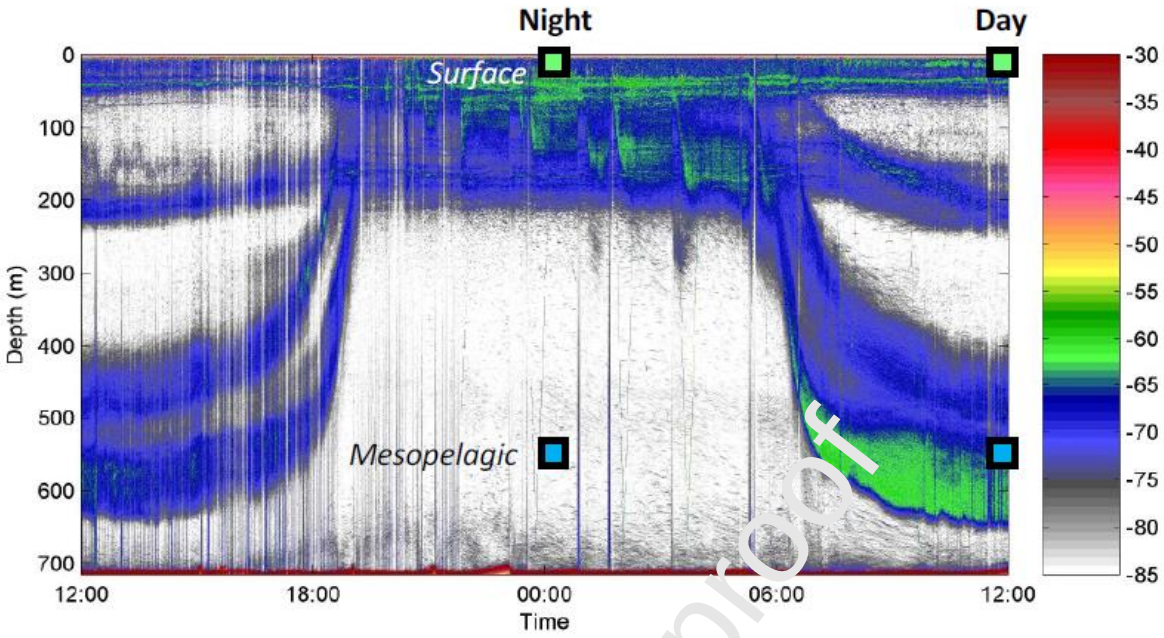

Fig. 1

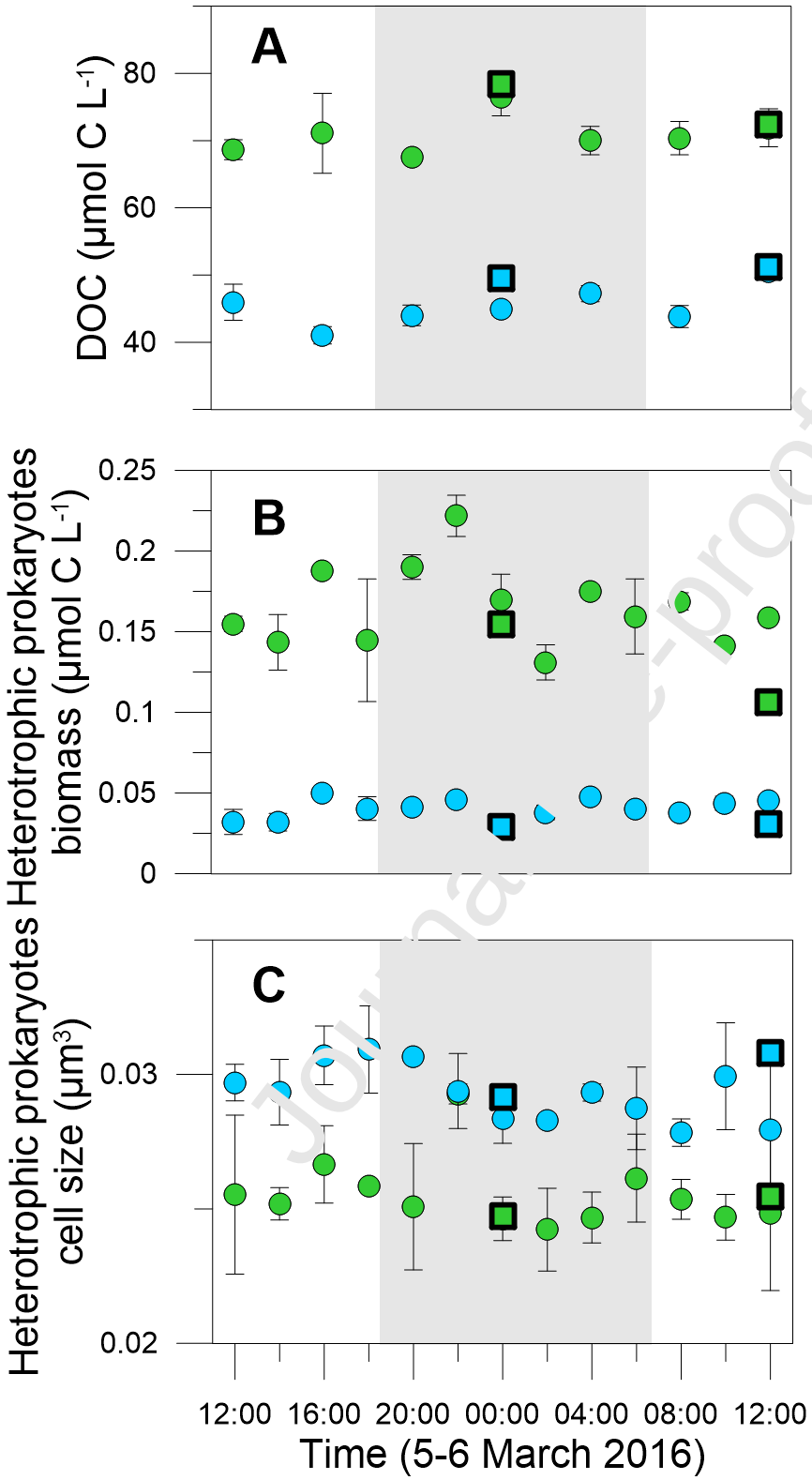
A
B
C
DOC (µmol C L-1)
Heterotrophic prokaryotes biomass (µmol C L-1)
Heterotrophic prokaryotes cell size (µm3)
80
60
40
0.25
0.2
0.15
0.1
0.05
0
0.03
0.02
12:00
16:00
20:00
00:00
04:00
08:00
12:00
Time (5-6 March 2016)

Fig. 2

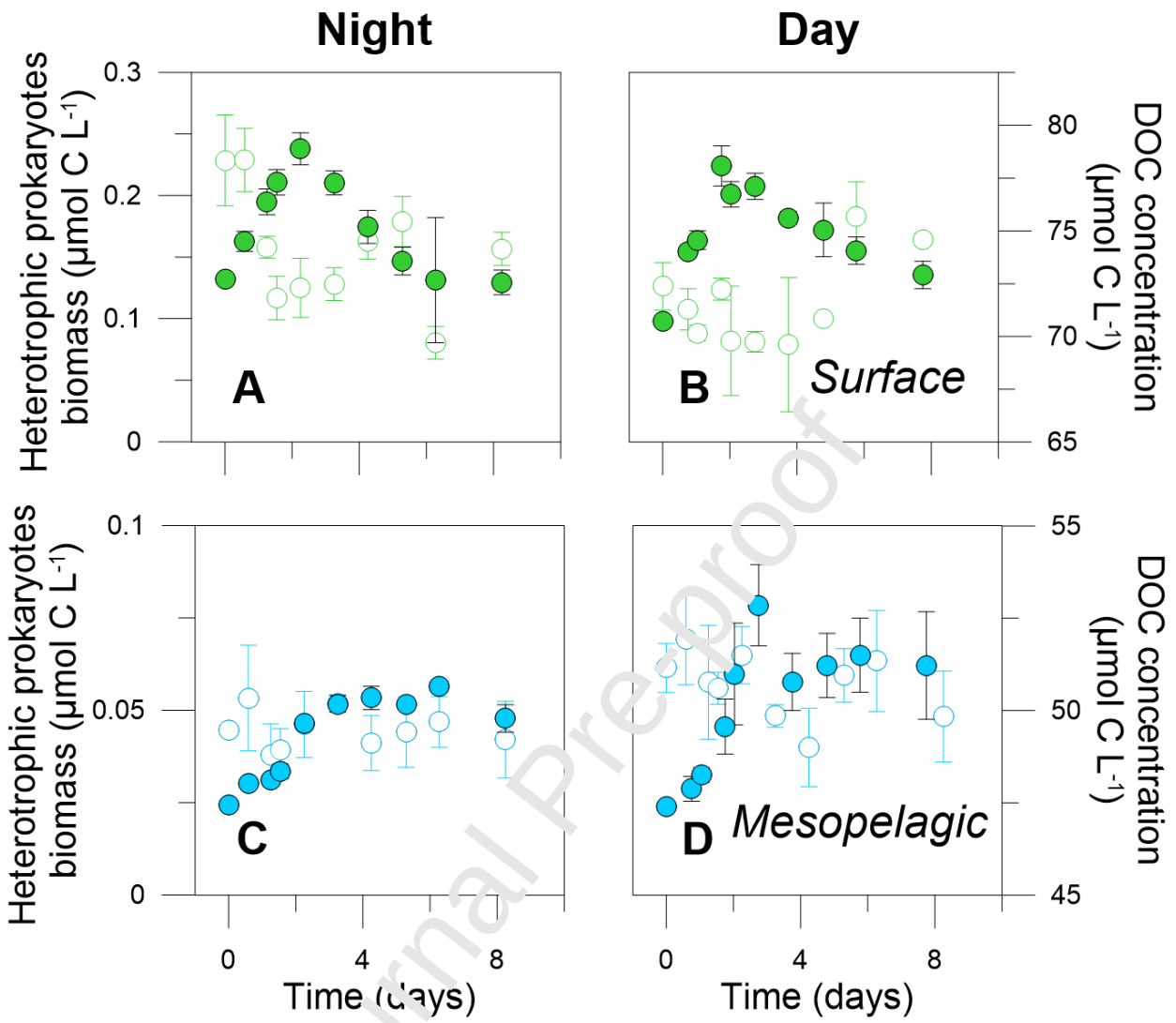

Fig. 3

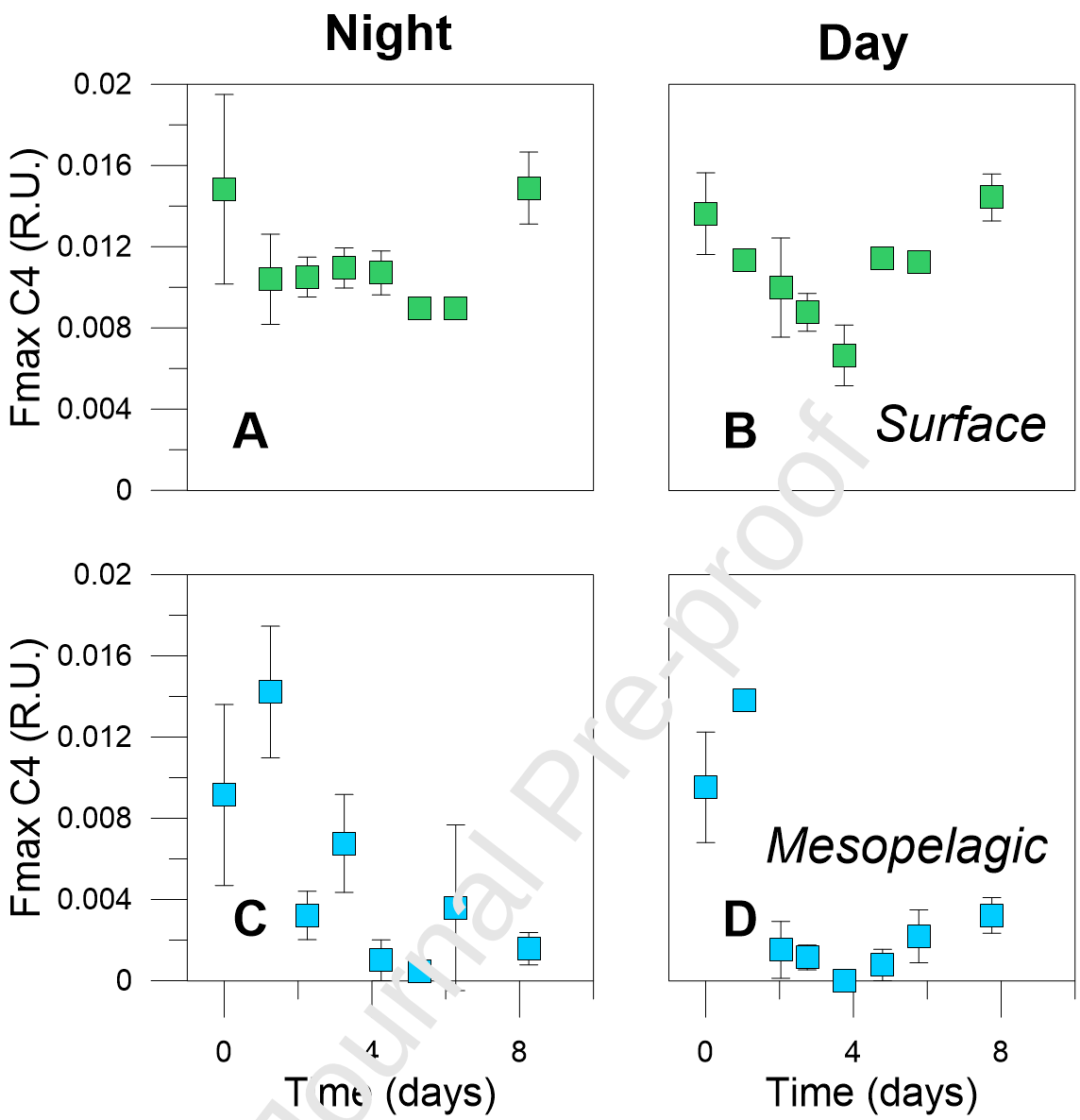

Fig. 4

Table 1. Mean ± SE values of specific growth rates (μ), DOC consumption rates or prokaryotic carbon demand (PCD, see the text), prokaryotic heterotrophic production rates (PHP) and prokaryotic growth efficiency (PGE) in the surface and mesopelagic layer incubation experiments performed at noon (Day) and midnight (Night). Rates were calculated for each period of exponential growth, also indicated in days. The same period was used for DOC consumption and biomass production rates. Also indicated are the maximum heterotrophic prokaryotes biomass reached within the incubation and the corresponding ratio of maximum to initial biomass (Max:t0 biomass ratio).

Layer	Time	Period (d)	μ (d^{-1})	DOC consumption rate (μmol C L^{-1} d^{-1})	PHP rate (μmol C L^{-1} d^{-1})	PGE (%)	Maximum HP biomass (μg C L^{-1})	Max:t0 HP biomass ratio
Surface	Day	0-1.75	0.34 ± 0.07	1.0 ± 0.5	0.040 ± 0.004	4.2	2.69 ± 0.20	2.30
	Night[a]	0-2.25	0.18 ± 0.02	2.7 ± 1.1	0.047 ± 0.006	1.8	2.85 ± 0.16	1.80
Mesopelagic	Day[a]	0-2.75	0.16 ± 0.04	0.5 ± 0.3	0.020 ± 0.004	4.2	0.94 ± 0.13	3.27
	Night	0-2.25	0.09 ± 0.01	0.3 ± 0.8	0.010 ± 0.001	3.1	0.68 ± 0.02	2.31

[a]Vertically migrating mesopelagic fish present

CRediT AUTHORSHIP CONTRIBUTION STATEMENT — Morán et al. STOTEN 052821

Xosé Anxelu G. Morán, Conceptualization, Methodology, Investigation, Formal analysis, Visualization, Writing - original draft, Project administration. **Francisca C. García**, Methodology, Investigation, Formal analysis, Writing - review & editing. **Anders Røstad**, Methodology, Formal analysis, Writing - review & editing. **Luis Silva**, Methodology. **Najwa Al-Otaibi**, Methodology. **Xabier Irigoien**, Investigation, Writing - review & editing. **Maria L. Calleja**, Methodology, Investigation, Formal analysis, Writing - review & editing.

Declaration of interests

☒ The authors declare that they have no known competing financial interests or personal relationships that could have appeared to influence the work reported in this paper.

☐The authors declare the following financial interests/personal relationships which may be considered as potential competing interests:

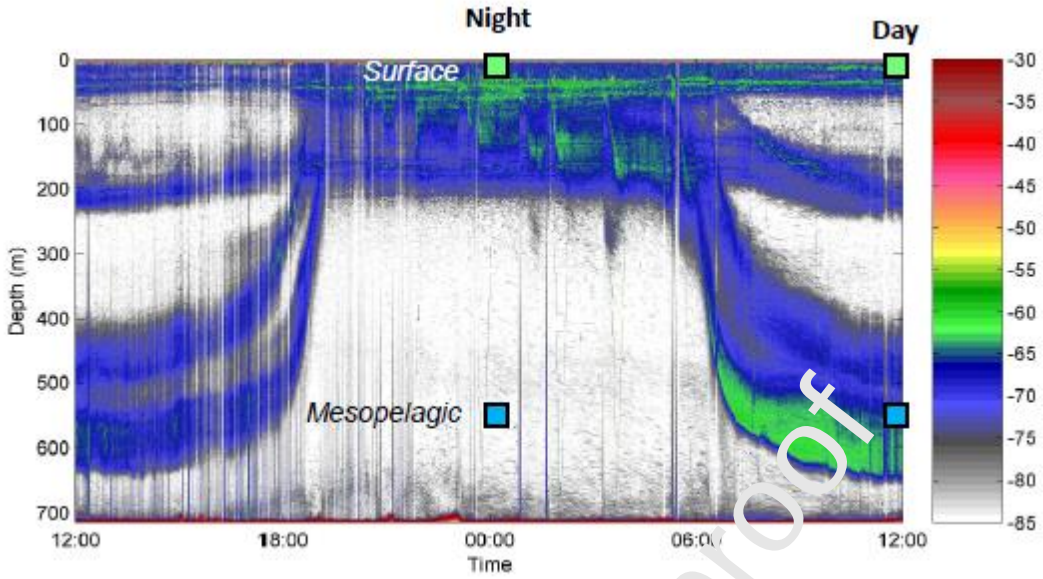

Graphical abstract

Highlights

- Diel cycles of DOM-heterotrophic prokaryotes interactions also occur in the mesopelagic zone
- Vertically migrating mesopelagic fishes release high quality DOM during daytime
- Incubation experiments and observations every 2 h demonstrate strong differences between day and night
- Larger heterotrophic prokaryotes grew longer and more efficiently with fishes present